AFFORDABLE QUASI THREE-DIMENSIONAL INVERSE DESIGN METHOD FOR PUMP IMPELLERS

by

Hans Spring

Hydrodynamics Specialist

Imo Industries Inc., Delaval Turbine Division

Trenton, New Jersey

Hans Spring graduated as a Mechanical Engineer in Switzerland (1951) and came shortly thereafter to this country. He received additional graduate education at Brown, Lehigh, and Northeastern University.

In his first industrial position, he became interested in centrifugal pumps, especially with regard to hydraulic design. In the late 1950s, he apprenticed hydraulic design under Alexey Stepanoff.

In 1968, he joined the Delaval Turbine Division as a Hydrodynamics Specialist. During his lifelong involvement in this specialty, he built pumps small enough so that they could be carried with one hand. On the other side of this scale, he designed circulating pumps with capacities exceeding 200,000 gpm. On the high energy side of the pump business, he was responsible for the hydraulic design of single stage reactor feed pumps with power requirements as high as 16,000 BHP.

Mr. Spring authored four ASME papers and co-authored one International Pump Symposium paper, all dealing with hydraulic design of pumps. He is a member of Delaval's Turbine Division Research and Product Development Department. He is a registered Professional Engineer.

ABSTRACT

Traditionally, the hydraulic design of impellers has been more of an empirical art than a well defined engineering science. Because of that empiricism, new designs have been disappointing at times. Discussed here is a "new" method called inverse design, which is destined to turn this empiricism into a well defined engineering discipline. Through this method, the design intent of the impeller can be clearly defined and specified. Therefore, this method is also of great value to pump users. The basic idea of inverse design is almost 50 years old and comes now to maturity, because fast running internal impeller flow codes are presently available to execute the necessary calculations.

INTRODUCTION

Impeller vane layout has always been the center of the art in hydraulic design. For a given impeller profile, there are virtually a thousand ways a vane can be designed between inlet and outlet angles. Some of the possible vane shapes would be better, some would not be very good with respect to successful design. Identifying the better shapes with certainty has been an impossible task. Also, the methods of laying out impeller vanes varied greatly. As little as 40 years ago, inlet and outlet angles for a new impeller design would be merely connected with a circular arc. If the impeller had to be of the Francis type, the three-dimensional aspects would be developed on conical sections.

In the 1950s, the Kaplan/Stepanoff Error-Triangle Method [1] became widely known in this country. In Europe, Pfleiderer [2] introduced his point by point blade design method. Both methods made the layout process considerably more sophisticated, but they did not contribute much to identifying the "best" vane shape, whatever that was. Vane design was always a tedious process, that was carried out on a drawing board. The layout work was most often delegated to people with an artistic gift in understanding the truly three-dimensional aspect of impeller design.

However, there was never any guarantee that a new impeller design was totally successful. For that reason, impeller modelling is still popular. If a company has a successful hydraulic design for a certain specific speed, and if a new larger design called for the same specific speed, the original design is enlarged with the help of a model factor. Modelling generally works well; the new design will have characteristics similar to the original design. However, if the original design had an undetected flaw, it would be magnified in the new larger design. Occasionally, a threshold was exceeded when modelling was applied. The vane loads would become unduly high, or impeller/diffuser gaps were left too small on new designs. Also possibly NPSH requirements would increase beyond what the modelling laws indicated. For these reasons, new larger designs can end up with defects which were not evident in the base designs.

Designers usually accumulate their experience into databases. Databases often are more reliable than any direct calculations. The trouble with them is that one is never assured that new design is the "best" that could be obtained. Also, the use of another designer's database can harbor problems, because of intrinsic misunderstandings.

The inverse design method will change all that and transform the "art of design" into a well defined engineering discipline. This is not only important for designers, but also for pump users. The basic concepts of inverse design are easily understandable, and people buying pumps in the future will be able to understand the design intent of a pump, which is presently not the case.

HISTORY

The origin of inverse design of turbomachinery impellers is traceable to World War II, Germany, to Wernher Von Braun's group of engineers and scientists that designed and built the V-1 and V-2 rockets. The writer first became aware of the idea in the early 1950s, when he was a research assistant at Brown University. A German professor taught a "Theory of Impeller Vane Design via Prescribed Averaged Circulation," in one of his turbomachinery classes. Viteri [3] presented a paper on computer aided design in 1983. This time the idea was coupled with a NASA internal flow code. After seeing the concept of inverse design for the second time, this writer was finally able to appreciate the tremendous potential of the method. Apparently, the inverse design method was able to survive since World War II within American aerospace companies. To the best of this author's knowledge, Viteri's paper was the first that was ever published on the subject of circulation

design. The writer undertook a five year development project which eventually ended up in a completely automated design procedure for impellers.

Within the past few years, there has been a flurry of papers published on the same subject. The papers of Borges [4] and Ghaly and Tan [5] are directly attributable to Hawthorne of Cambridge, England. Independent of the German origin, Hawthorne had come upon the idea of inverse design by a specified mean swirl. Mean swirl has the same meaning as specified average circulation. Hawthorne concentrates on developing fully three-dimensional codes for the inverse design of impellers. This is in contrast to this presentation where a quasi three-dimensional internal flow code was selected [6]. The main advantage of a quasi 3-D code is that it's running time is much shorter than a fully 3-D code. Furthermore, at this time, fully 3-D codes for inverse design are not commercially available, and can only handle special applications, whereas the selected quasi 3-D code is applicable to all impeller specific speeds, with and without inlet prerotation.

There is also a different inverse design method which is becoming well known. It is based on the original work of Stanitz [7]. The vane shape is calculated from a prescribed velocity distribution. Bonataki, et al. [8], have developed the idea to the level of a quasi three-dimensional cascade calculation, which is applicable to all turbomachinery type impellers. Also, Al-Zubaidy [9] has successfully applied this method to the design of high pressure compressor impellers. Both Bonataki and Al-Zubaidy use quasi 3-D codes for the numerical procedures.

METHODOLOGY

The mathematical aspects in this presentation are kept to an absolute minimum and only those items which are absolutely necessary to understand the principle are discussed. Equation (1) is the Euler equation which describes the head of a pump with 100 percent efficiency and no slip.

$$H\,(EULER) = \frac{1}{g} \cdot [U2 \cdot CU2 - U1 \cdot CU1] \qquad (1)$$

Equation (2) shows Pfleiderer's slip modification to the Euler equation. The theoretical head corresponds to a pump with 100 percent hydraulic efficiency and the slip has been accounted for.

$$H\,THEO = \frac{H\,(EULER)}{(1+P)} = \\ \frac{1}{g\,(1+P)} \cdot [U2 \cdot CU2 - U1 \cdot CU1] \qquad (2)$$

Equation (3) is Equation (2) with the slip division carried out. In executing this division, the slip cannot be applied to the incoming flow conditions of the impeller that is represented by U1 and CU1. Also, the slip has no effect on U2, the outlet peripheral velocity. Therefore, only CU2 can be affected, which is recognized by substituting CU22 for CU2 in Equation (3). (For simplicity several steps between Equations (2) and (3) have been purposely omitted.)

$$H\,THEO = \frac{1}{g} \cdot [U2 \cdot CU22 - U1 \cdot CU1] \qquad (3)$$

As described in Equation (4), the formation of theoretical head evolves along a streamline in the impeller, with the end condition at the impeller exit as expressed in Equation (3).

$$H\,THEO\,(M) = \frac{1}{g} \cdot [U(M) \cdot CU(M) - U1 \cdot CU1] \qquad (4)$$

In the APPENDIX, there is a short definition for the circulation and how it applies to pump impellers. The final result of the APPENDIX is reflected in Equation (5). In Equation (4), the angular velocity Omega can be bracketed out, which yields Equation (6). Now the expressions within the brackets in Equation (6) and Equation (5) are identical.

$$\Gamma = [\Gamma\,(M) - \Gamma\,1] = 2\pi \cdot [R(M) \cdot CU(M) - R1 \cdot CU1] \qquad (5)$$

$$H\,THEO\,(M) = \frac{\omega}{g} \cdot [R(M) \cdot CU(M) - R1 \cdot CU1] \qquad (6)$$

Substituting Equation (5) into Equation (6) gives Equation (7), which expresses the theoretical head as a function of the circulation.

$$H\,THEO\,(M) = \frac{\omega}{2\pi g} \cdot [\Gamma\,(M) - \Gamma\,1] \qquad (7)$$

Equation (7) is also of great practical value to the reader, because the impeller circulation can be viewed as merely being proportional to the theoretical head. For a really easy grasp of the situation, the reader can equate the circulation as being the same as the pump head.

The question of how circulation can be used to design a new impeller blade shape is addressed in Figure 1. The solid lines in Figure 1 represent a velocity triangle somewhere within an impeller located at [M] on a streamline. Because of the existing vane design, an absolute velocity C, a relative velocity W, a tangential velocity CU, a peripheral velocity U, and a meridional velocity CM are generated. These quantities define the flow angle BF2. The component CU at [M] defines a certain amount of circulation, as shown in Equation (4).
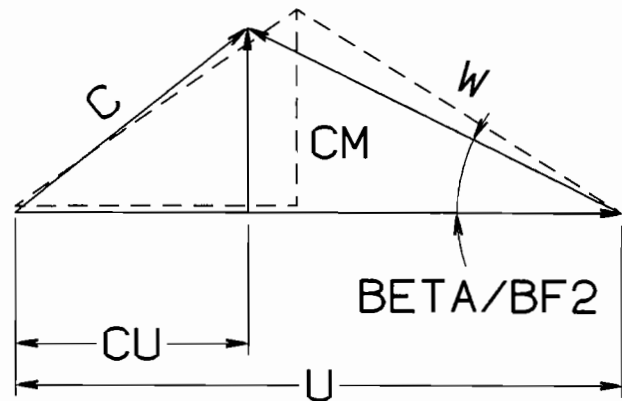

Figure 1. Circulation Design of a New Impeller Blade Shape.

The dashed lines describe a different flow triangle at the same location, when a larger circulation is specified. The new dashed line velocity triangle corresponds to a larger flow angle. This process is carried out at many points within an impeller employing small changes only for each iterative calculation. When this calculation is finished, the blade angles within the impeller are changed, and a new blade shape has emerged, according to the newly specified circulation (which later will be referred to as "circulation standard").

The change that has taken place locally under the influence of a newly specified circulation standard is represented in Figure 1. It is also evident that the meridional velocity CM could change. All of these calculations take place at a large number of points, which

makes it necessary to use a computer. A quasi three-dimensional code has been adopted for this purpose [6].

The fluid velocity components CU and CM located on a certain radius, R, are varying between blade to blade in a pitch-wise direction. It is generally true that these components averaged in the pitch-wise direction correspond to the blade shape at that location. This holds true throughout most of the impeller except for the inlet area, if there is any flow deviation and near the outlet area, where the impeller slip occurs. It is for this reason that this type of inverse design calculation is referred to as "averaged specified circulation."

TWO DESIGN EXAMPLES

Impeller A

In order to illustrate how the design method works, two design examples are discussed. Before an inverse method for vane design can be used, an impeller profile has to be established, as is shown in Figure 2. The impeller hub diameter DH is dictated by the shaft diameter, which is obtained from rotordynamic considerations. The impeller eye diameter, D1, can calculated with reasonable confidence [10]. The impeller discharge diameter, D2, can be approximated by several well known methods [1, 2, 11, 15]. The impeller discharge width, B2, is best established through a ratio of B2/D2 as a function of specific speed from a database. The shroud radius, RS, has to be made as large as possible, as conditions permit. There are many good recommendations as to the axial length of the meridional profile [17]. The inlet angles can be estimated from a 1984 article [10], or any other source. Exit angle Beta2 comes from a database as a function of specific speed.
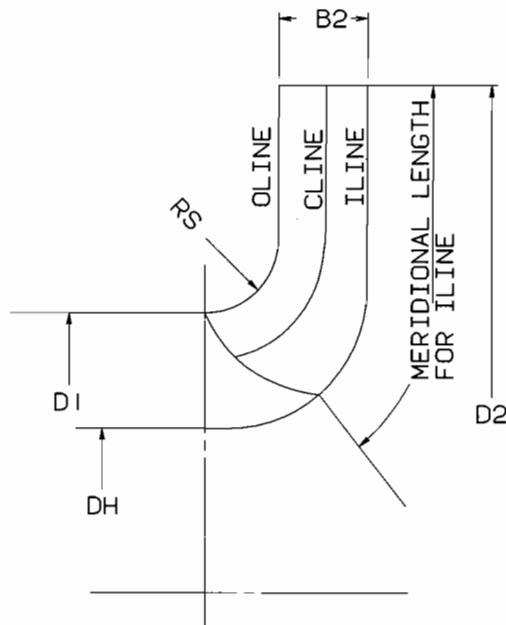

Figure 2. Impeller Profile.

The profile defined in Figure 2 is for a hypothetical boiler feed pump stage designed for a specific speed of 1400. This profile is used for both design examples. The first impeller design shall be denoted as impeller A. The circulation standard chosen for impeller A is depicted in Figure 3. The ordinate of this graph represents the circulation in percent and the abscissa represents the absolute meridional length of the profile for the I-line, C-line, and O-line. I-line stands for inside line (hub), C-line stands for center line, and O-line stands for outside line (shroud). The inlet to the impeller is

at the right hand side of the graph at locations 4 to 5. The exit of the impeller is at location 0 at 100 percent circulation. The specified circulation lines describe the head buildup in the impeller along the three major streamlines. The circulation requires that the head buildup be steady from the inlet and eventually be slightly moderated near the outlet of the impeller. The circulation distribution was assumed to be a reasonable requirement for a boiler feed pump interstage. The circulation standard uniquely specifies an impeller blade shape. It is not possible that two different blade shapes can satisfy one type of circulation. The next step is to carry out the calculations to find the blade shape that corresponds to the circulation in Figure 3. A skeleton view of the resulting impeller design is shown in Figure 4. On the left hand side of Figure 4, the previously chosen impeller profile appears again. On the right hand side of Figure 4 is an end view of the impeller blade. The vane has relatively little twist and the angular wrap is short.
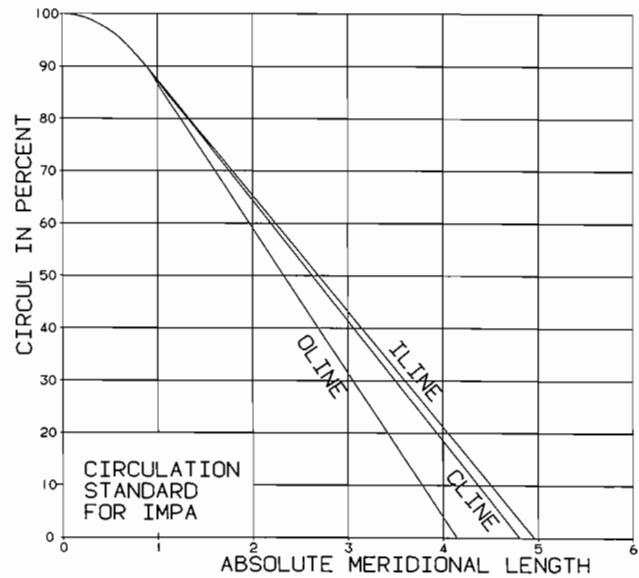

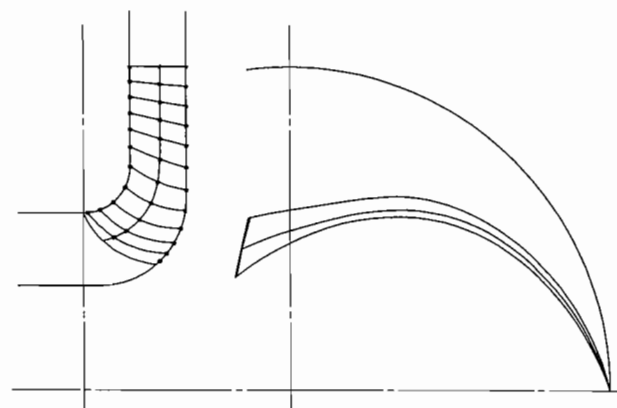Figure 3. Circulation Standard for Impeller A.

Figure 4. Impeller A.

A multiple parameter view is shown in Figure 5 of the results from the inverse design calculations for the I-line, for the best efficiency capacity. The abscissa again corresponds to the meridional length with the inlet to the impeller located approximately at location 14. The impeller exit is at location 1. Shown on this graph
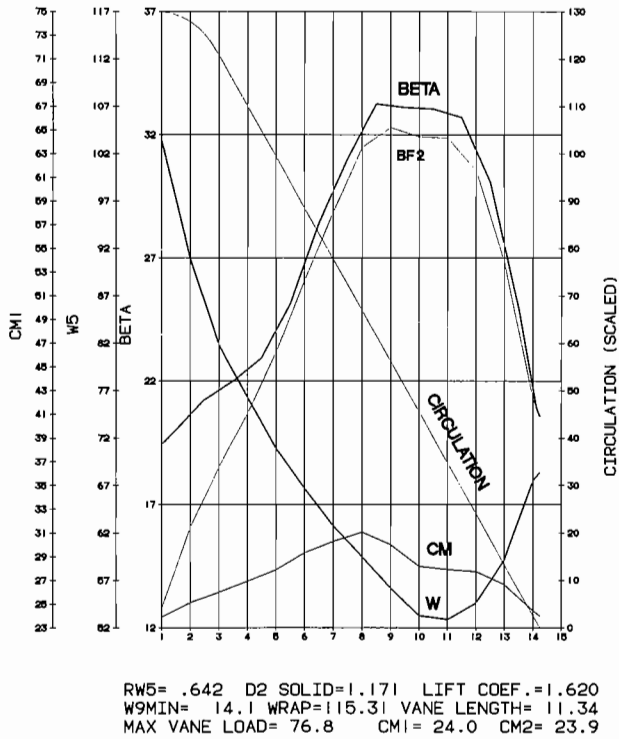
RW5= .642 D2 SOLID=1.171 LIFT COEF.=1.620
W9MIN= 14.1 WRAP=115.31 VANE LENGTH= 11.34
MAX VANE LOAD= 76.8   CMI= 24.0 CM2= 23.9

Figure 5. I-Line, Impeller A.

is a reproduction of the circulation which goes approximately diagonally through the graph. Note that the circulation signature rises steeply from the inlet and is slightly moderated near the exit exactly like the circulation standard.

The inlet blade angle to the impeller, Beta1, is located above location 14. The blade angles increase sharply to a maximum of about 34 degrees and then turn down to the exit at location 1 with an exit angle Beta2 of 20 degrees. As indicated in Figure 5, the impeller wrap at the I-line is 115.31 degrees. This is a small wrap. The blade is short because of the rapid increase of impeller angle from the inlet. The rapid increase of the impeller blade angles is dictated by the sharp increase of the circulation near the inlet.

The fluid flow angles BF2 are examined next. At the inlet, there is no flow deviation. At location 5, the impeller flow angle starts to deviate from the impeller blade angle. This is the location where the quasi 3-D code indicates the beginning of the impeller slip. Also pictured is the relative velocity W; it's shape is dictated by the vane angles. Essentially, the relative velocity changes smoothly from the inlet to the outlet. The author has analyzed many impellers for their circulation signature and has found that sometimes relative velocities have several dips until they finally reach the exit. The circulation design method is an excellent tool to design impellers that have also smoothly changing internal relative velocities. The C-line or center line is represented in Figure 6. Generally, all remarks made for the I-line apply here, also. There is no deviation angle between the impeller blade angle Beta and the fluid flow angle BF2 at the inlet. The O-line or outside line for impeller A is shown in Figure 7. Again, there is no deviation angle on the inlet impeller. The circulation is exactly replicated, as given on the standard, and the relative velocity, W, is smoothly distributed throughout the streamline.

From the data discussed so far, it is not possible to determine whether this is a good or a bad design. However, in the caption of Figure 7, the O-line, the lift coefficient is listed as 1.558. The lift coefficient is a measure derived from vane length and circulation, and is too high for the impeller (Equation (8)).

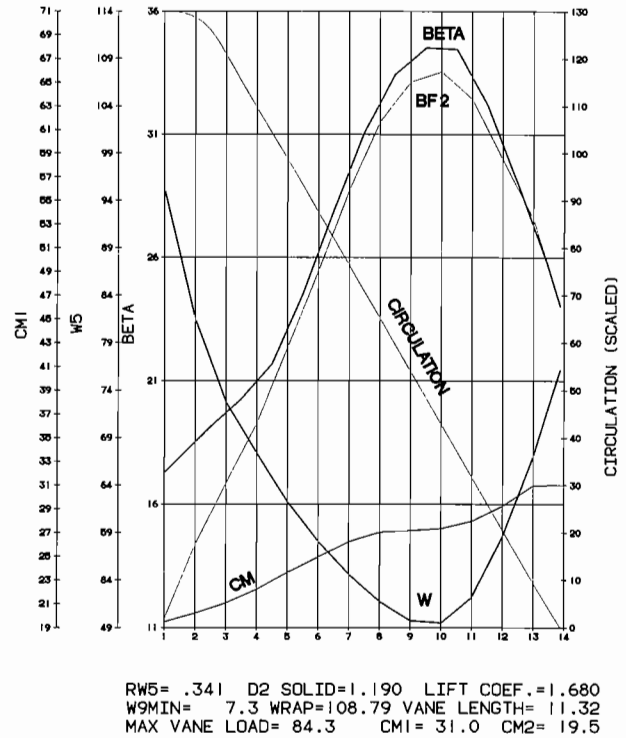$$\text{LIFT COEF.} = \frac{2 \cdot \Gamma}{\left(\dfrac{W1 + W2}{2}\right) \cdot ZI \cdot VL} \tag{8}$$

RW5= .341 D2 SOLID=1.190 LIFT COEF.=1.680
W9MIN= 7.3 WRAP=108.79 VANE LENGTH= 11.32
MAX VANE LOAD= 84.3   CMI= 31.0 CM2= 19.5

Figure 6. C-Line, Impeller A.

RW5= .498 D2 SOLID=1.201 LIFT COEF.=1.558
W9MIN= 16.6 WRAP=103.00 VANE LENGTH= 11.21
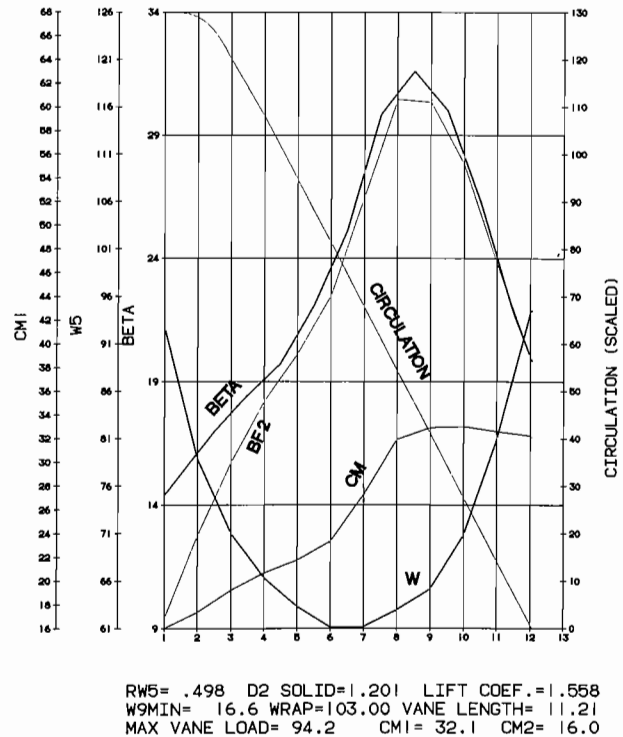MAX VANE LOAD= 94.2   CMI= 32.1 CM2= 16.0

Figure 7. O-Line, Impeller A.

The ordinate on Figure 8 is the blade surface relative velocity on the three major streamlines. The upper velocity represents the suction side velocity and the lower velocity represents the pressure side velocity of the vane. The abscissa corresponds to the meridional length. As indicated previously, the circulation chosen for this impeller starts with a steep angle near the inlet, requiring a lot of head buildup fast. As a result, the inlet of the blade, which is at the left hand side of each graph, experiences heavy velocity loading. It has been pointed out already that this velocity loading takes place with no flow deviation angle at the inlet. Therefore, the high velocity loading near the inlet, is the result of the chosen circulation.

The blade velocity loading coefficient is represented in Equation (9). The limits for this coefficient are often given as 0.7 to 1.5. Looking at the caption below the graphs, it is seen that the blade loading coefficients for the I-line, C-line and O-line are 1.256, 1.699, and 1.42, respectively. Obviously, the center stream line exceeds the recommendation of 1.5.

$$\text{BLADE VEL. COEF.} = \frac{(\text{W SUCT.}) - (\text{W PRESS.})}{(\text{W AVG.})} \quad (9)$$

So far, it has been established that the lift coefficient in the O-line is too high, and that the blade load coefficient in the center line is too high. The fact that the impeller is loaded heavily near the inlet, is not necessarily a bad condition. However, the overriding consideration for rejecting this impeller design is that the pressure side minimum blade velocity on all three stream lines is only approximately 10 ft/sec. This impeller would work perfectly well at the best efficiency point, but not at lower flows. Impellers are designed at the best efficiency point, and certain features have to be included to make their operations at low capacities acceptable. Because of the low pressure side velocities, it can be concluded that this impeller would start to stall very close to the best efficiency point. In other words, the rotating stall would commence maybe at 90 percent capacity. The result would be a drooping characteristic at shutoff.

The pressure loading of impeller A is represented in Figure 9. The pressure distribution on the suction and pressure side of the impeller has been calculated from the velocities shown on Figure 8. Very high pressure loading of the O-line and the C-line inlets is indicated. The major downfall of impeller A was caused by the requirement that the circulation should start with a steep angle near the inlet. The blade pressure coefficient shown in Figure 10 is after
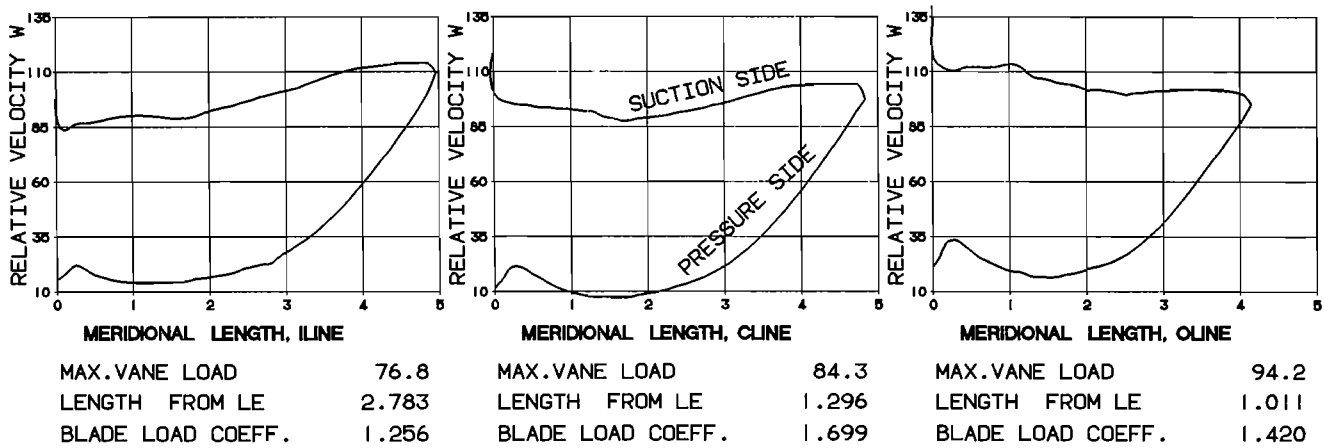

MAX.VANE LOAD	76.8	MAX.VANE LOAD	84.3	MAX.VANE LOAD	94.2
LENGTH FROM LE	2.783	LENGTH FROM LE	1.296	LENGTH FROM LE	1.011
BLADE LOAD COEFF.	1.256	BLADE LOAD COEFF.	1.699	BLADE LOAD COEFF.	1.420

Figure 8. Relative Loading of Impeller A.

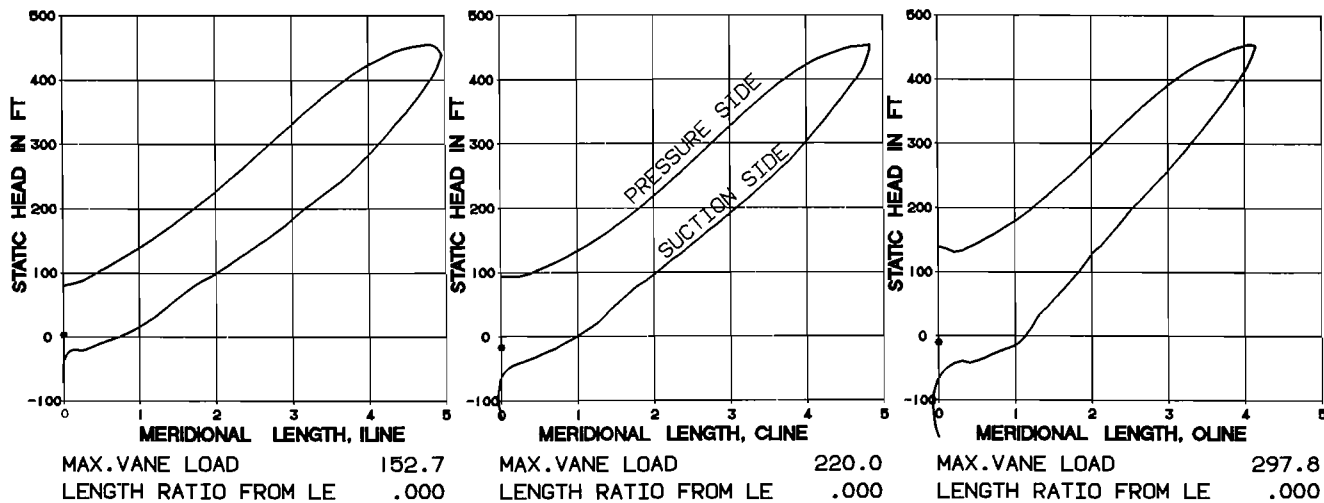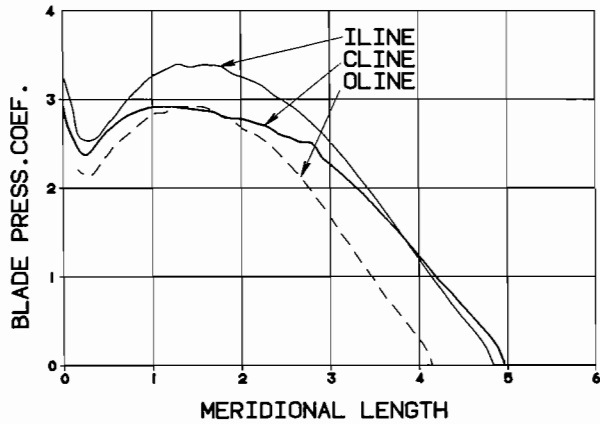| MAX.VANE LOAD	152.7	MAX.VANE LOAD	220.0	MAX.VANE LOAD	297.8
LENGTH RATIO FROM LE	.000	LENGTH RATIO FROM LE	.000	LENGTH RATIO FROM LE	.000

Figure 9. Static Head of Impeller A.

Morris and Kenny [12], as defined in Equation (10). Discussion of the diagram is deferred until the results of impeller B are examined.

$$\text{BLADE PRESS. LOAD'G} = \frac{(H\ PRESS) - (H\ SUCT.)}{\dfrac{(W\ AVG.)^2}{2g}} \quad (10)$$

ILINE:	MAX.BLADE LDG.COEFF.	2.923
CLINE:	MAX.BLADE LDG.COEFF.	3.398
OLINE:	MAX.BLADE LDG.COEFF.	2.948

Figure 10. Blade Pressure Coefficient of Impeller A.

Impeller B

Impeller B uses the same meridional profile as impeller A. The chosen circulation standard for impeller B is represented in Figure 11. All three circulation lines begin with much smaller angles than the corresponding ones for impeller A, which will result in less loading near the inlet. Also, the circulation is a straight line near the exit, which causes heavier loading at that location (as compared to impeller A). However, the impeller diffusion will be less. The circulation specified in Figure 11 results in a skeleton blade shape, as indicated in Figure 12. It is apparent that the wrap of this
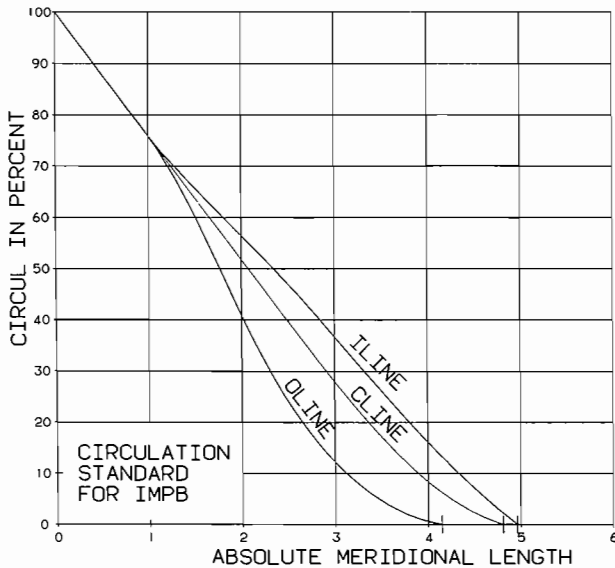

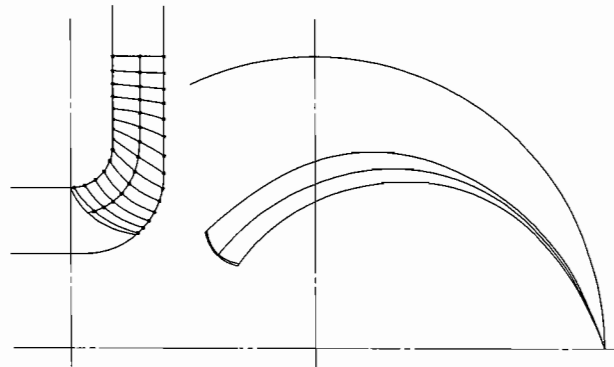Figure 11. Circulation Standard for Impeller B.

Figure 12. Impeller B.

impeller is larger than the wrap of the first impeller. Also, the twist of the blade is considerably more than on impeller A.

The C-line parameter data is shown on Figure 13. The inlet blade angle near location 14 is approximately 23 degrees. The blade angle starts to increase to approximately 25 degrees, which is considerably less than on impeller A. This is a direct result of the moderation of the circulation near the impeller inlet. The total wrap of the impeller at the centerline is approximately 136 degrees. The relative velocity distribution is also smooth from inlet to outlet. The O-line for impeller B is presented in Figure 14. The Beta distribution is very uneven, but the relative velocity is rather smoothly distributed. This is quite in contrast to a design that was done with the Kaplan/Stepanoff Error-Triangle Method. That method generally results in a very smooth Beta distribution and an irregular relative velocity. It should be obvious that a smoothly changing relative velocity distribution in an impeller is more important than a smoothly changing blade angle distribution. The lift coefficient in the O-line is 1.252, which is quite acceptable.
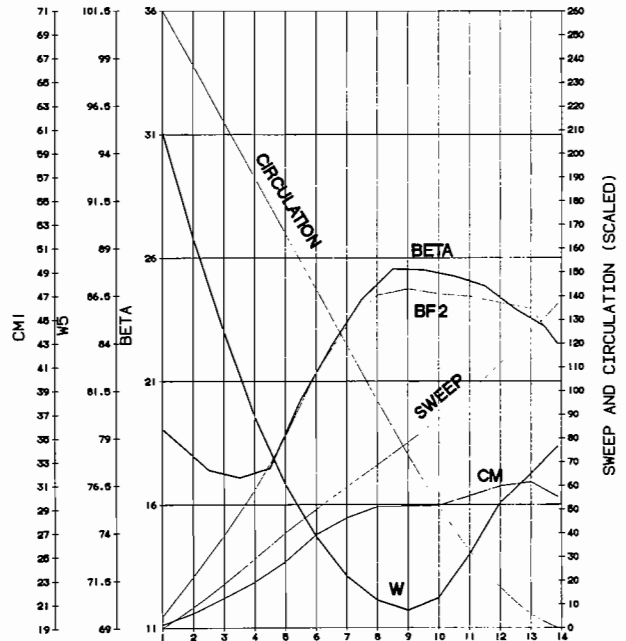
RW5= .588 D2 SOLID=1.323 LIFT COEF.=1.394
W9MIN= 34.3 WRAP=135.99 VANE LENGTH= 13.45
MAX VANE LOAD= 70.7   CMI= 30.0 CM2= 19.3
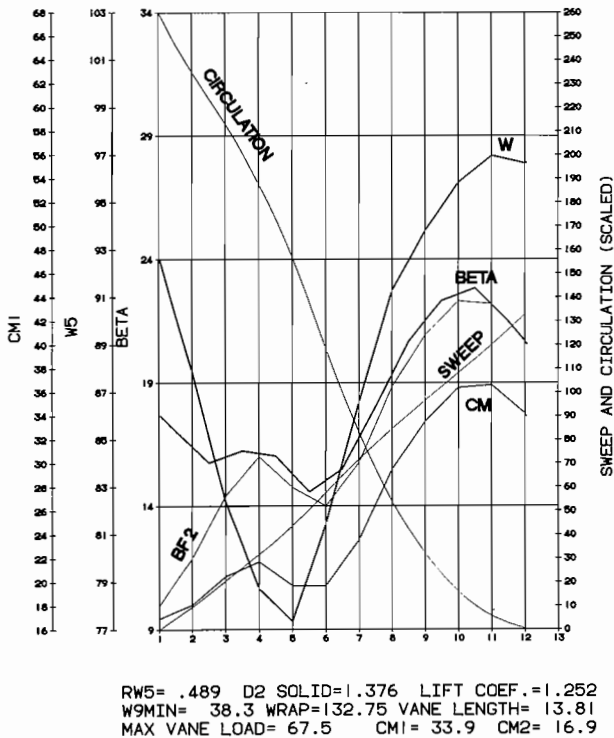
Figure 13. C-Line, Impeller B.

RW5= .489 D2 SOLID=1.376 LIFT COEF.=1.252
W9MIN= 38.3 WRAP=132.75 VANE LENGTH= 13.81
MAX VANE LOAD= 67.5   CMI= 33.9 CM2= 16.9

Figure 14. O-Line, Impeller B.

The blade velocities for impeller B are described in Figure 15. The velocity loading near the inlet is much less than for impeller A. The circulation was chosen to produce an approximately uniform blade pressure loading. It is not known whether this is a very favorable condition, but the circulation design method permits an exact specification where this loading is desired. The blade velocity loading coefficient is roughly 0.9 to 1.0, which is considerably less than the loading condition obtained on impeller A. This impeller is relatively lightly loaded in comparison to many other designs, and therefore, the customary range for this specification, 0.7 to 1.5, appears to be too broad. The minimum pressure side velocity W9MIN in the shroud equals 38 ft/sec. Therefore, there is no concern that the beginning of the rotating stall is very close to the best efficiency point.

The O-line diffusion can be defined through Equation 11.

$$RW5 = \left| \frac{W \; MIN}{W \; MAX, \; INLET} \right|_{PRESSURE \; SIDE} \qquad (11)$$

The lowest pressure side velocity is divided by the highest pressure side velocity near the inlet, which yields 0.489 and is a good value. This is one of the most important aspects of the hydrodynamic design with regard to low flow capabilities of an impeller. As the water flows along the first half of the vane pressure side, its velocity is being reduced in an increasing pressure field. If this diffusion rate is too large, than the flow will separate away from the wall and eventually stall. Hence, if the diffusion is minimized in the shroud, the stall strength can be reduced, which is a most beneficial condition for a good head curve shape at low flows. The portion of the pressure side, where the velocity increases, poses no problem. For pumps, the suction side velocity (the upper velocity) never appears to pose a particular problem with regard to diffusion, because the velocities are either increasing or stay approximately horizontal.

The pressure loading of impeller B is depicted in Figure 16. The lightest loading is generally at the inlet and the overall loading is evenly distributed. The Morris Kenny blade pressure coefficient of impeller B is shown in Figure 17. This compares to Figure 10 of impeller A. The maximum O-line blade loading coefficient for impeller B is 1.87 as compared to the corresponding number of 2.948 for impeller A. Both impellers produce approximately the same head. If the pressure loading coefficient for the shroud can be made lower, then the low flow characteristics of the impeller will improve. The peak in Figure 17 is lower and occurs later than in Figure 10. Morris recommends that the pressure loading coefficient should not be higher than 0.7. Morris is a compressor designer, and this possibly is an inherent difference between a compressor impeller and a pump impeller, even though the design methods now are continuously approaching.

The circulation standard for impeller B, because of a straight exit, produced a better shroud diffusion rate than the circulation for impeller A, which was moderated toward its exit. However, it must be noted that the relative blade loading near the exit of impeller B, Figure 15, is considerably higher than the corresponding exit loading of impeller A in Figure 8. Any resulting pump performance changes can only be established through actual tests.

It is worth mentioning that designers Kovats [15] and Yedidiah [16] have long advocated that the exit impeller angle Beta2 is of no great consequence in an impeller design. This is contradictory to established theories, where the exit Beta2 angle is a cornerstone of the design assumption. It is noted that all the exit angles of impeller
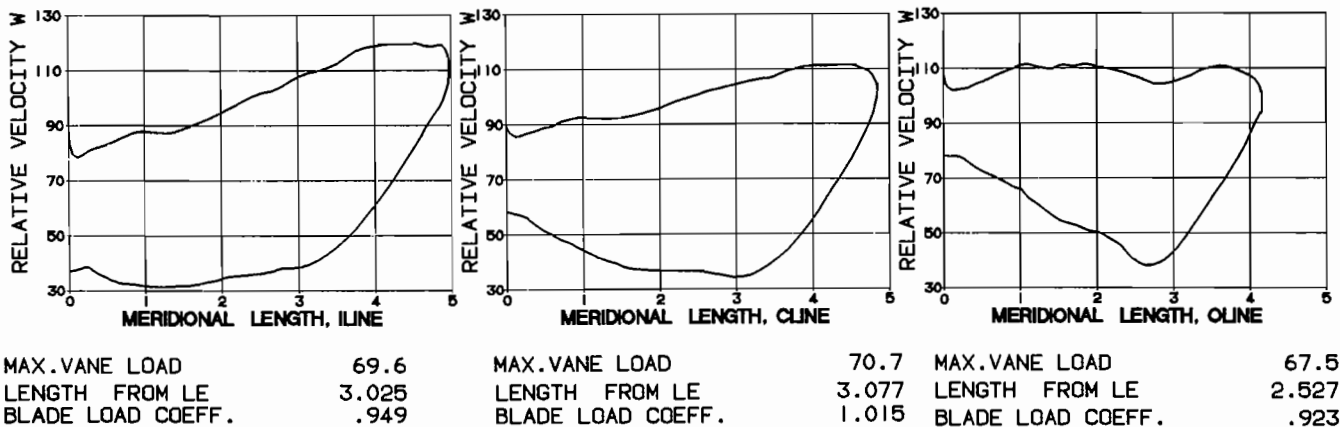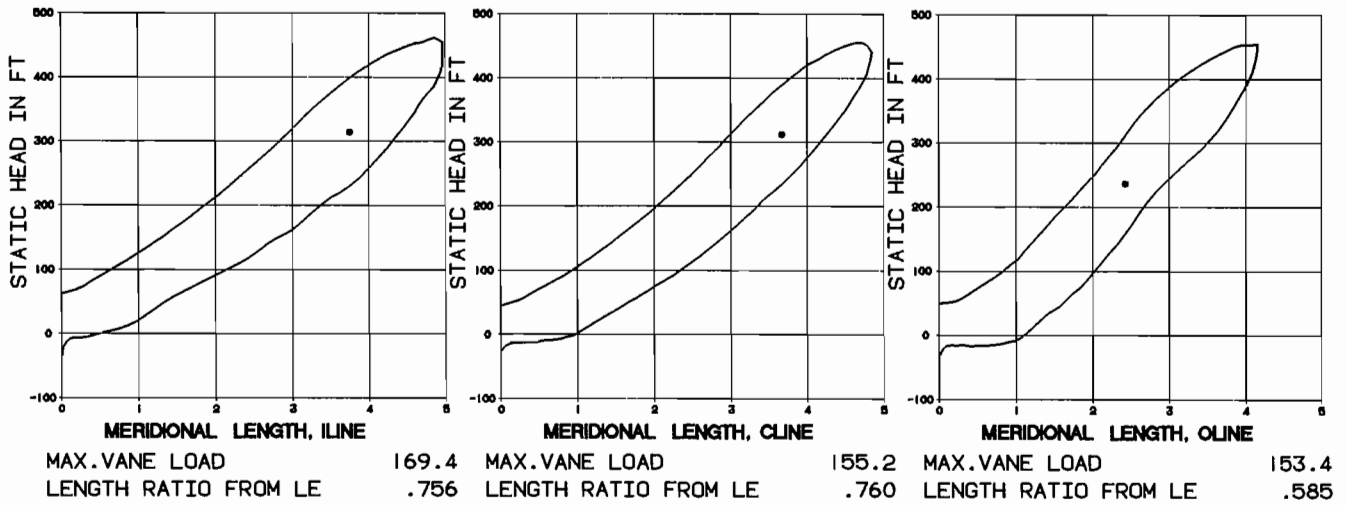

MAX.VANE LOAD	69.6	MAX.VANE LOAD	70.7	MAX.VANE LOAD	67.5
LENGTH FROM LE	3.025	LENGTH FROM LE	3.077	LENGTH FROM LE	2.527
BLADE LOAD COEFF.	.949	BLADE LOAD COEFF.	1.015	BLADE LOAD COEFF.	.923

Figure 15. Relative Loading of Impeller B.

| MAX.VANE LOAD | 169.4 | MAX.VANE LOAD | 155.2 | MAX.VANE LOAD | 153.4 |
| LENGTH RATIO FROM LE | .756 | LENGTH RATIO FROM LE | .760 | LENGTH RATIO FROM LE | .585 |

Figure 16. Static Head of Impeller B.

ILINE:	MAX.BLADE LDG.COEFF.	1.904
CLINE:	MAX.BLADE LDG.COEFF.	2.030
OLINE:	MAX.BLADE LDG.COEFF.	1.871
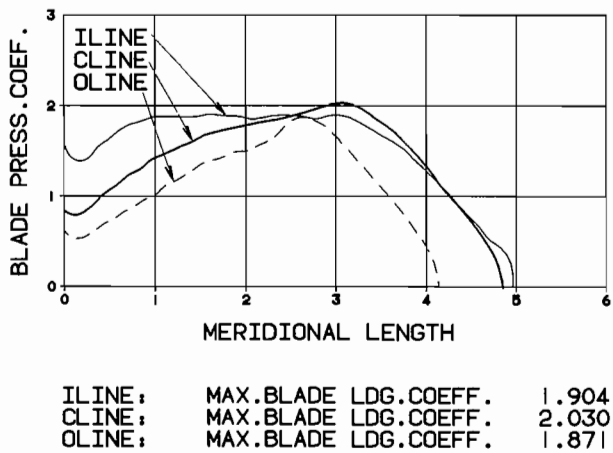
Figure 17. Blade Pressure Coefficient for Impeller B.

A and B have different values. The TE Beta2 angles are defined by the specified circulation. The total Beta angle distribution is more important than the actual Beta2 angle.

THE CIRCULATION OF A SUCCESSFUL SUCTION IMPELLER

Impeller C

A very successful suction impeller for boiler feed pumps is shown in Figure 18. Its flow is rated for 10,700 gpm at 2200 ft with a speed of 5075 rpm. It reaches a suction specific speed of 14,485 at three percent head drop. This type of impeller has been running in boiler feed pumps successfully for a period of more than 12 years. It was not designed with inverse design methods. The circulation signature is shown on Figure 19. Had the impeller been designed with the inverse method, it would have been possible to choose smooth circulation lines in order to produce uniform internal velocities. The O-line circulation has a very light loading near the pump inlet. The I-line circulation near the inlet starts with a steep angle. The corresponding blade velocity loadings for impeller C is shown in Figure 20. The inlet velocity loading is extremely light in the O-line, while it is very heavy in the I-line, as defined already by the circulation signature. Figure 21 is the pressure loading of the impeller. Note the light pressure loading in the shroud line and the heavy pressure loading in the hub line near

the inlets. The black areas below the zero Static Head Line on the head scale indicate a major portion of the NPSH requirement of the impeller. The black area in the shroud is considerably less than the black area in the hub. The NPSH requirements of this impeller in the hub are much larger than in the shroud because of the heavy loading of the hub line. When this impeller was originally tested
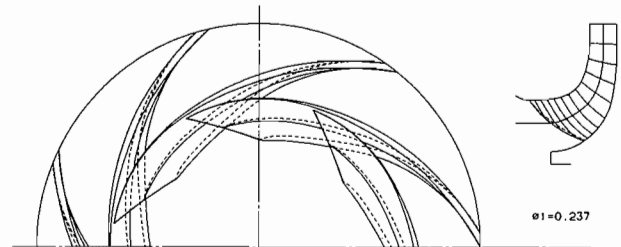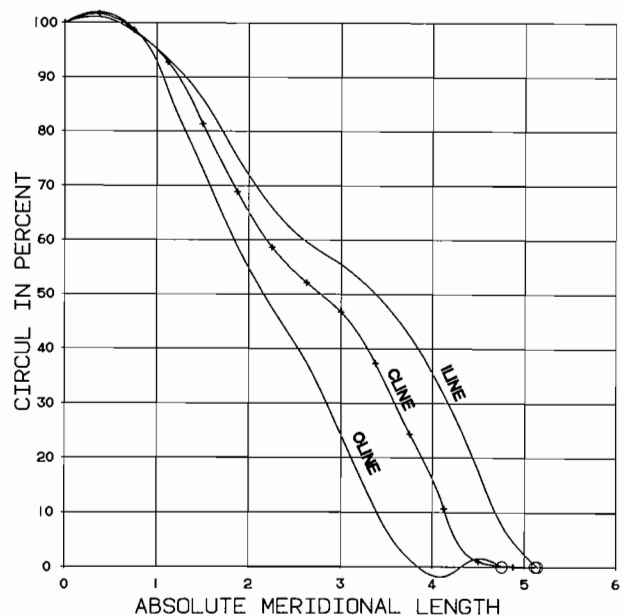

Figure 18. Impeller C.

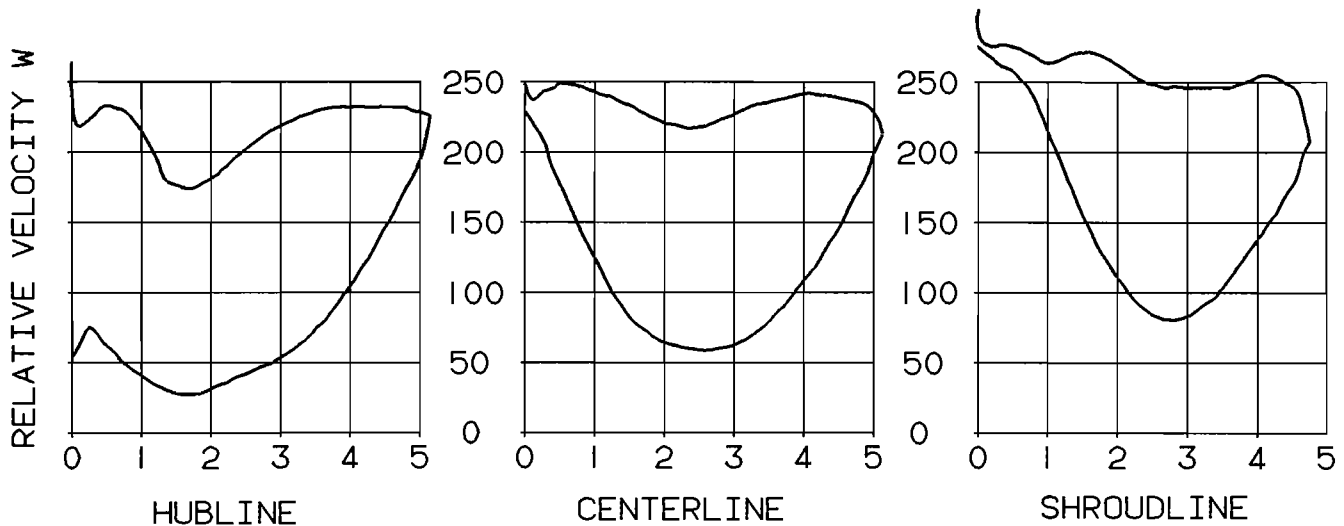*Figure 19. Circulation from Impeller C.*

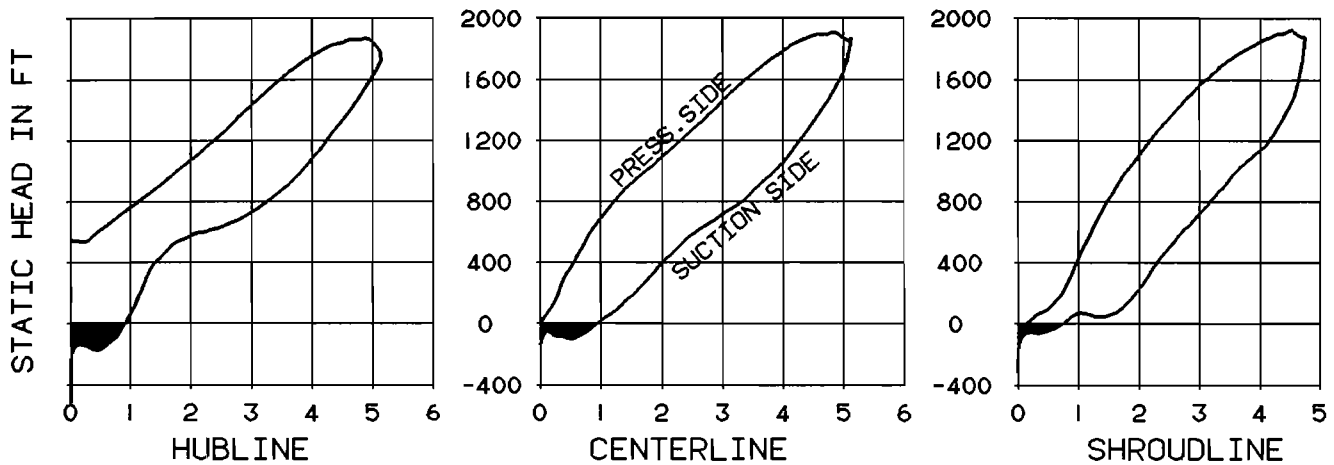Figure 20. Blade Velocity Loading of Impeller C.

Figure 21. Static Head Rise of Impeller C.

for cavitation, it was found that the first cavitation bubbles started to form near the hub. Details of this impeller and other suction impellers appear in the literature [13].

Even though this is a superior suction impeller, it would have been possible to improve its design using the inverse design method.

THE IMPORTANCE OF THE SHROUD'S DIFFUSION ON OFF PEAK PERFORMANCE

Impellers are designed for the best efficiency point. If everything is calculated properly, one can expect a good efficiency. However, impellers must operate at low flows also. During the design, certain characteristics have to be incorporated, that will assure that the impeller has acceptable low flow characteristics. Drooping curves at shutoff are not acceptable. One of the most important design parameters is the shroud diffusion rate. The results of two different boiler feed pump stage tests are shown n Figure 22. The head scale for the characteristic curves is shown in an exaggerated condition, so that the effects of the shroud's diffusion rate can be better highlighted. Impeller D is represented by the dashed lines and has a shroud diffusion rate of 0.1, which is a common value found on pumps of this kind. The characteristic curve has a flat spot occurring around 1500 gpm and from then on

climbs toward the shutoff of roughly 770 ft. Impeller E has a shroud diffusion rate of 0.4, and is shown with solid lines. It does not have a flat spot at 1800 gpm, it is merely a change in slope. At shutoff, the head rises to approximately 830 ft. Both impellers had the same profile and outside diameter. The difference in shutoff head was achieved solely through a different blade shape in impeller E with a better diffusion rate along the shroud. Below roughly 1800 GPM, the brakehorsepower curve of impeller E is above the brake horsepower curve of impeller D. This is a visual demonstration that the rotating stall strength in impeller E is weaker than in impeller B. This can be explained in the following way: In impeller D, at 1500 gpm, there is a rapid change in pump head. This is approximately the location where the full rotating stall has emerged in front of the impeller (vortex motion in front of impeller eye). The back flowrate and the strength of the stall are such that the ability of the impeller to do more work is impaired. At the same 1500 gpm, impeller E generates more head and consumes more brakehorsepower; a sign that the rotating stall (vortex) must be weaker. The rotational component of the stall is not as large as in impeller D, therefore, impeller E can do more work in that location and other locations. Paradoxically, the lesser stall begins at a larger flow for impeller E, mainly around 1800 gal. The same phenomena for volute pump impellers has been reported by Schiavello [14].
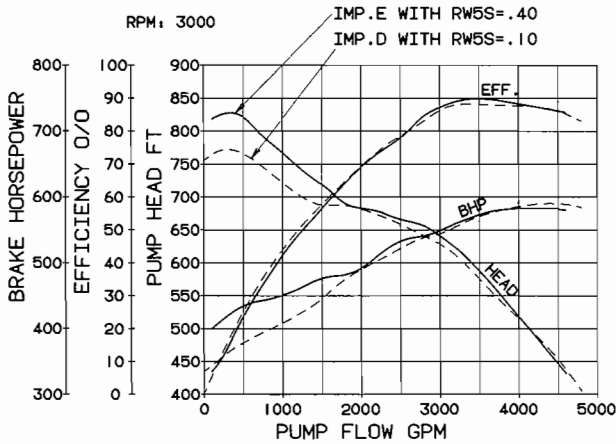
Figure 22. Effect of Shroud Diffusion Rate.

Figure 23. Impeller F.

APPLICATION

There was one opportunity to apply the method to a large revamp pump design. Some twenty years ago, the company had received an order for six circulation pumps for 97,500 gpm flow each. These pumps are of double suction design with a specific speed of 5100. Each pump is driven by a 3000 hp motor. Due to the size of the pumps, they could not be tested at the factory at the time of shipment, nor could they be adequately tested at the customer's installation. However, it was known that they fulfilled the customer's pumping requirement within the available hp envelope of the electric motors. Several years ago, the customer required more flow, which was met by underfiling these impellers. Then the customer found he needed more flow yet, and asked for a revamp impeller design. This was a good opportunity to apply the inverse design method. It was proposed to the customer that the existing design would first be analyzed with the now available analysis and design tools and a definitive answer would be issued after that was accomplished. For the computer analysis, the original "stick-off" drawings that the pattern makers used for the original impeller were employed to assure accuracy.

The impeller F, which represents the original design, is portrayed in Figure 23. The drawings on Figure 23 were automatically generated through computer graphics from the design data. This impeller, almost 50 in in diameter, had originally been laid out by the Kaplan/Stepanoff design method on a drawing board. Impellers of that specific speed are particularly hard to lay out, because hub and shroud are on curved surfaces. Twenty years ago, a layout man labored on this project for a minimum of two weeks, trying to come up with a suitable blade shape that matched specified inlet and outlet angles. Today, a similar drawing can be done by a computer in seconds. The circulation signature obtained from existing impeller F is shown in Figure 24. Looking at the O-line, it is seen that the circulation first turns negative. That is equivalent to the impeller working first as a turbine, and then as a pump. This is an indirect answer to the earlier raised question: What is the best vane shape? Obviously, the conventional design methods do not provide that information. Most impeller designs of that age suffer from defective circulation at one point or another, because internal flow codes were not available back then. The C and I-line circulation starts with relatively steep angles, which results in heavy loading of the impeller inlet. The circulation lines are particularly wavy which indicates undesirable velocity variations. The blade velocity loading is shown in Figure 25. There is relatively heavy loading at the I-line, medium loading at the C-line, and at the O-line, the impeller does not produce any useful work near the entrance, as already indicated by the circulation signature.
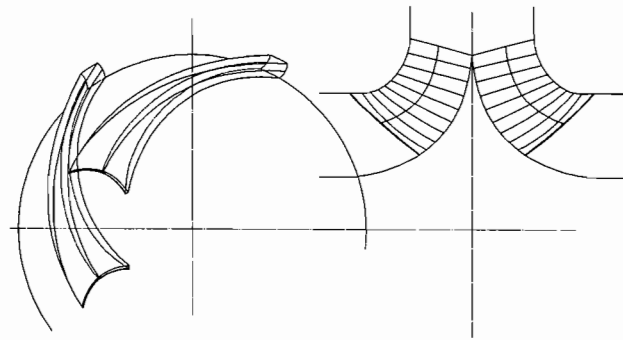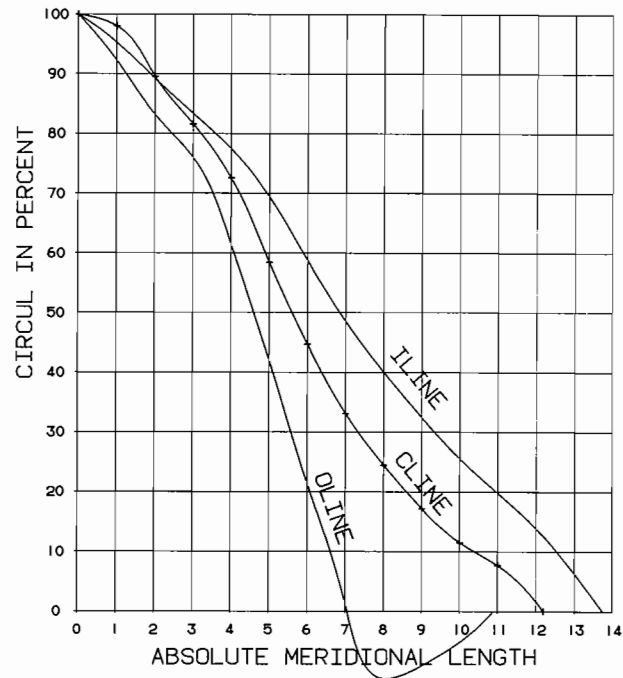

Figure 24. Circulation from Existing Impeller F.

The pressure loading of impeller F is represented in Figure 26. There is a substantial NPSH requirement for the I-line and the C-line, the suction pressure is considerably below zero at the inlet of the impeller. In the O-line, no effective work takes place until after location 2. The pressure load coefficient according to Morris is represented in Figure 27. Deliberation will be deferred until impeller G has been discussed.

The customer was informed that the flow of the existing pumps with a retrofit impeller could be increased. The customer responded with an order for two impellers. The circulation standard shown in Figure 28 was used for the blade design for revamp impeller G. The main difference of this circulation vs the one from impeller F is that all three circulation lines start with lightly loaded conditions near the impeller inlet, which is located at 100 percent. The circulation lines are essentially straight lines that are moderated toward the exit. The resulting impeller G design is indicated on Figure 29. The only obvious difference is the shape of the leading edge, which is a straight line now. Otherwise, the impeller drawing does not reveal any changes that are visible to the eye. However, the impeller is quite different than original impeller, based on the performance indicators. The velocity loading of the impeller is imaged in Figure 30. Although impeller G is designed
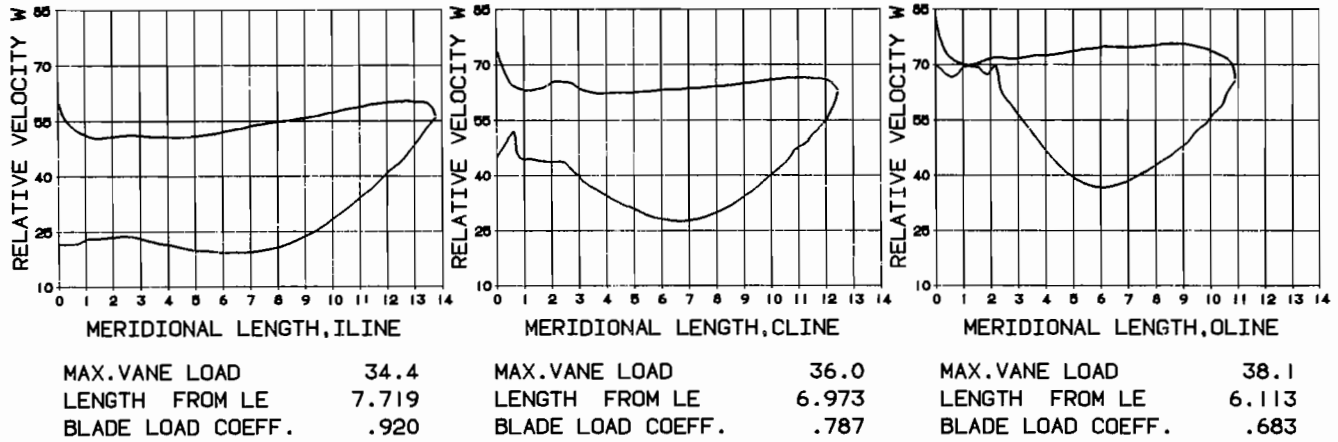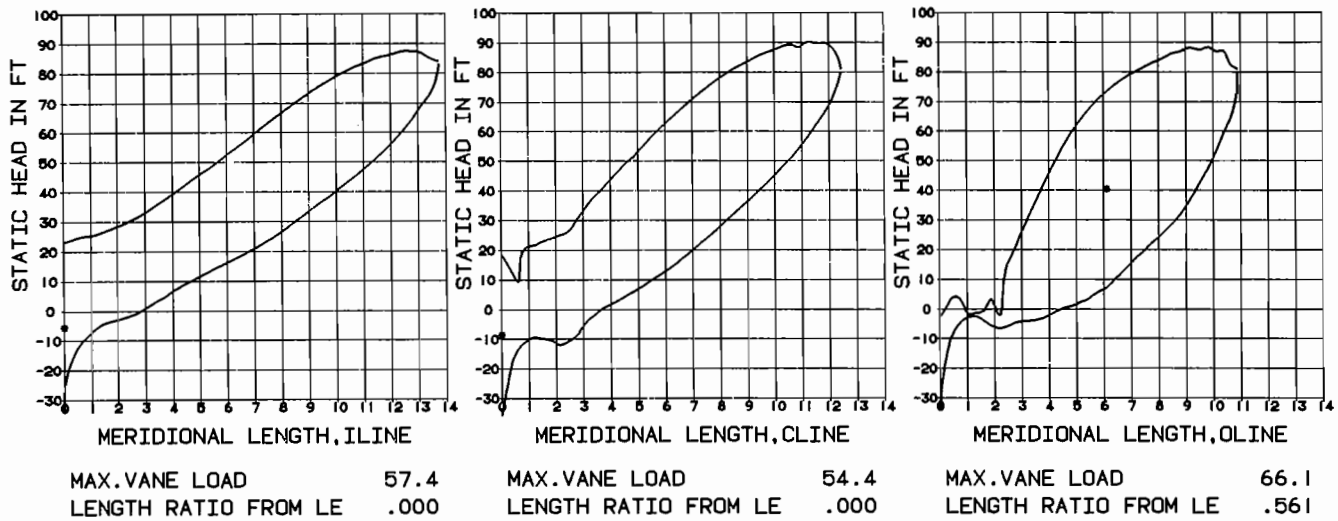
MAX.VANE LOAD	34.4	MAX.VANE LOAD	36.0	MAX.VANE LOAD	38.1
LENGTH FROM LE	7.719	LENGTH FROM LE	6.973	LENGTH FROM LE	6.113
BLADE LOAD COEFF.	.920	BLADE LOAD COEFF.	.787	BLADE LOAD COEFF.	.683

Figure 25. Relative Loading of Impeller F.

| MAX.VANE LOAD | 57.4 | MAX.VANE LOAD | 54.4 | MAX.VANE LOAD | 66.1 |
| LENGTH RATIO FROM LE | .000 | LENGTH RATIO FROM LE | .000 | LENGTH RATIO FROM LE | .561 |

Figure 26. Static Head of Impeller F.

ILINE:	MAX.BLADE LDG.COEFF.	1.999
CLINE:	MAX.BLADE LDG.COEFF.	1.576
OLINE:	MAX.BLADE LDG.COEFF.	1.365
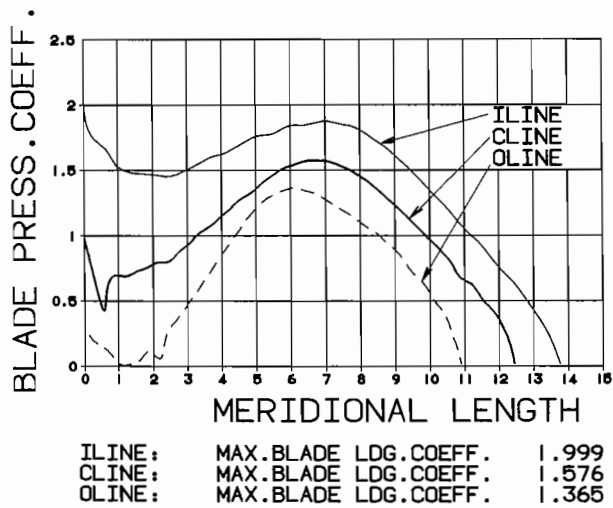
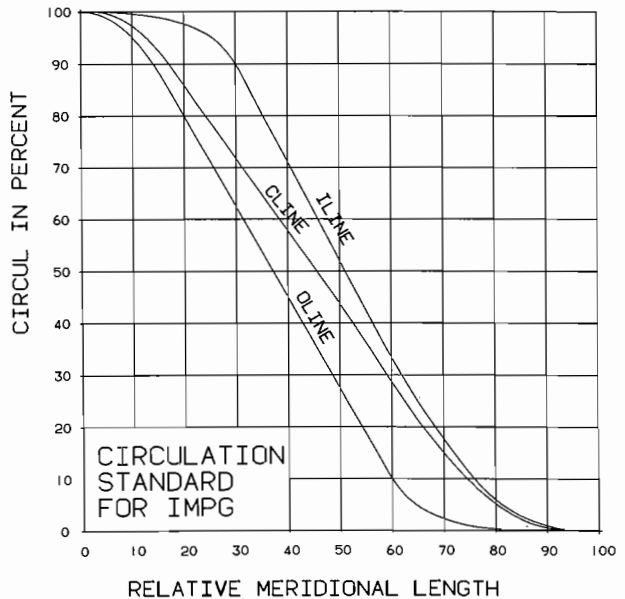*Figure 27. Blade Coefficient for Impeller F.*

for 19 percent more flow without any modifications to the pump case, the blade loading coefficients are mostly less than the ones

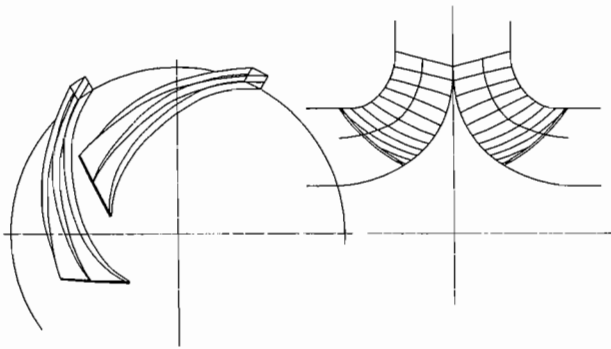*Figure 28. Circulation Standard for Impeller G.*

Figure 29. Impeller G.

from the original impeller. The velocity loading near the inlet of the three streamlines is now considerably less than in the original impeller. Had the blade taper (profiling) at the O-line been made longer, then the inlet loading on the O-line would be even less than indicated now. The NPSH requirements are also reduced as indicated in Figure 31. (Suction side pressure below the zero level on the vertical static head scale). The Morris pressure loading coefficient for impeller G is displayed in Figure 32. The maximum coefficients for the C-line and O-line are slightly reduced, while

the coefficient in the I-line is approximately equal to the impeller F in Figure 27.

After installation of the impellers and an observation of nearly one and one-half years, the customer reported that the revamp flow was achieved with less power consumption than with the original impellers. The company received an order for four more impellers of the same type.

CONCLUSION

It is hoped that a good understanding of the tremendous power of the inverse design method has been conveyed. It was shown through the example of two boiler feed pump impellers A and B, that the exact blade shape could be generated through the selection of a circulation standard. Furthermore, it was seen that with the judicious selection of the circulation standards, the blade loading characteristics could be kept under complete control. This design control can be measured as lift coefficient, maximum vane velocity loading, the velocity loading coefficient at that point, and finally, the pressure loading coefficient as defined by Morris. It has been demonstrated that inverse design is capable of producing a blade shape, which in turn, yields the best possible diffusion rates.

In the case of suction impeller C, it was demonstrated that the circulation method can be used to define lightly loaded inlet conditions. For the given example, it was shown how this impeller
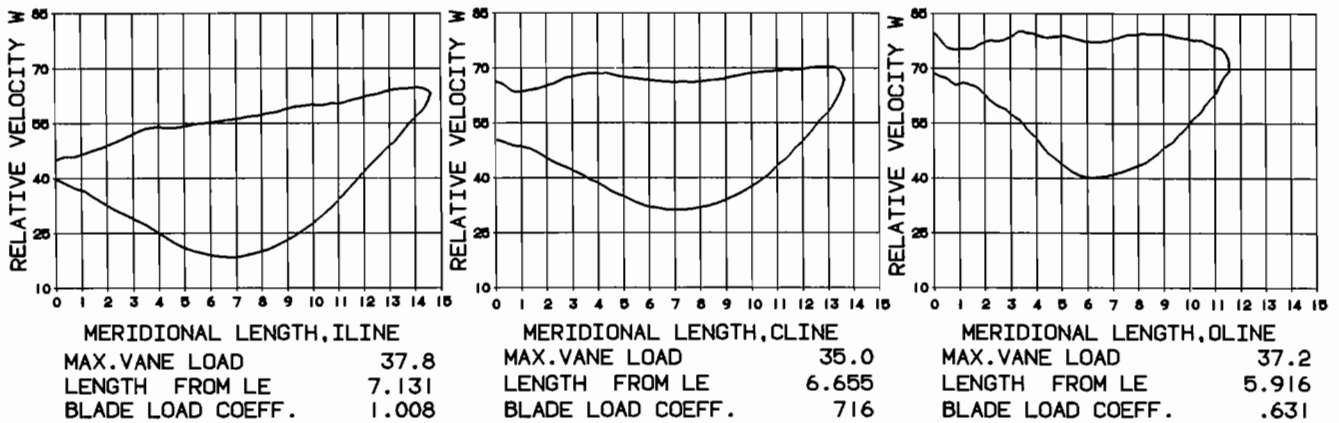

MERIDIONAL LENGTH, ILINE	MERIDIONAL LENGTH, CLINE	MERIDIONAL LENGTH, OLINE
MAX.VANE LOAD 37.8	MAX.VANE LOAD 35.0	MAX.VANE LOAD 37.2
LENGTH FROM LE 7.131	LENGTH FROM LE 6.655	LENGTH FROM LE 5.916
BLADE LOAD COEFF. 1.008	BLADE LOAD COEFF. 716	BLADE LOAD COEFF. .631

Figure 30. Relative Loading of Impeller G.

MERIDIONAL LENGTH, ILINE	MERIDIONAL LENGTH, CLINE	MERIDIONAL LENGTH, OLINE
MAX.VANE LOAD 45.7	MAX.VANE LOAD 53.3	MAX.VANE LOAD 69.7
LENGTH RATIO FROM LE .634	LENGTH RATIO FROM LE .441	LENGTH RATIO FROM LE .659

Figure 31. Static Head of Impeller G.

ILINE: MAX.BLADE LDG.COEFF.   2.016
CLINE: MAX.BLADE LDG.COEFF.   1.432
OLINE: MAX.BLADE LDG.COEFF.   1.263
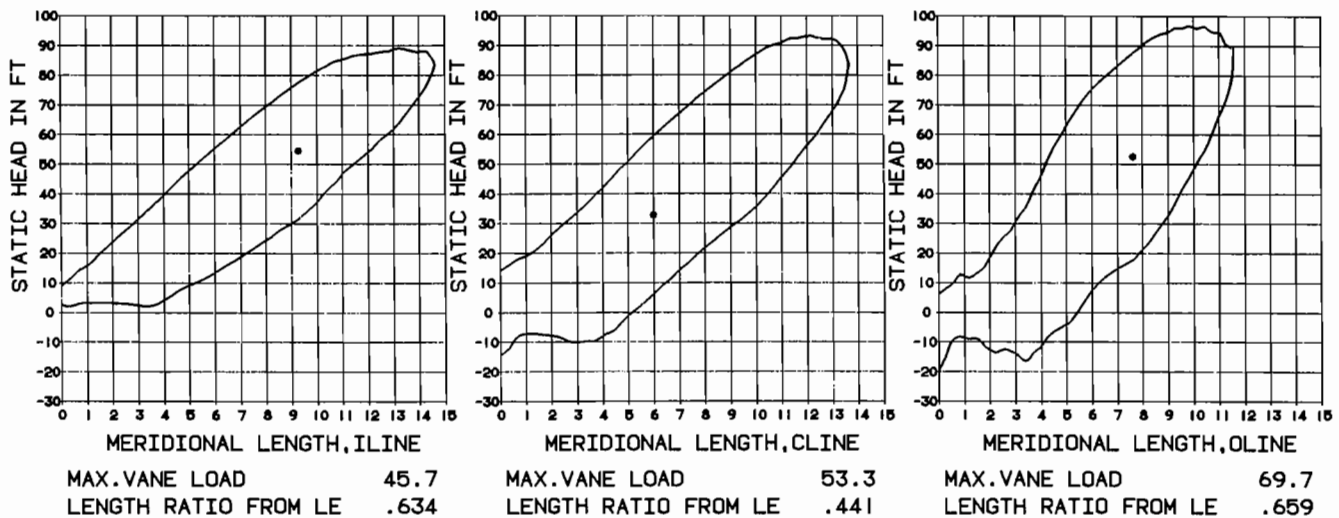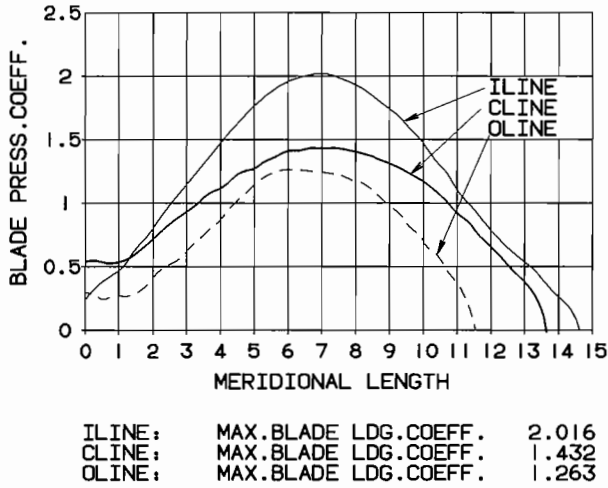
Figure 32. Blade Loading Coefficient for Impeller G.

could have been improved through the use of inverse design, even though this impeller has already reached a state-of-the-art suction specific speed.

The example of impellers E and D demonstrated the importance of the shroud diffusion rate on the off-peak performance. It has been shown that with inverse design, shroud diffusion rates can be generated that are not possible to obtain with conventional design methods. With the revamp example of impeller F and G, which was a first example of the application of the inverse design method, it was shown that it is possible to help increase a power plant's output through improvements to old existing pumps.

APPENDIX

Averaged Circulation in Impellers

The averaged circulation in an impeller at a particular location in a pitch-wise direction can be expressed as the line integral of the averaged tangential velocity component CU over the length (Figure A-1 and Equation (A-1)).

$$\Gamma = \oint C \cdot \cos \propto \cdot dl \qquad (A\text{-}1)$$

$$= \oint CU \cdot dl \qquad (A\text{-}2)$$

$$= \quad CU \oint dl \qquad (A\text{-}3)$$

Since CU is the averaged pitch-wise component, it can be set in front of the integral (A-3).

Equation (A-4) defines the circulation on a circle with radius, R, at a particular location, M, at an impeller streamline.

$$\Gamma (M) = CU(M) \cdot 2 \cdot R(M) \cdot \pi = 2\pi \cdot R(M) \cdot CU(M) \qquad (A\text{-}4)$$

Since an impeller can be designed with prerotation, then the circulation at the LE is defined by Equation (A-5).

$$\Gamma 1 = 2\pi \cdot R1 \cdot CU1 \qquad (A\text{-}5)$$

The total circulation at location M will be:

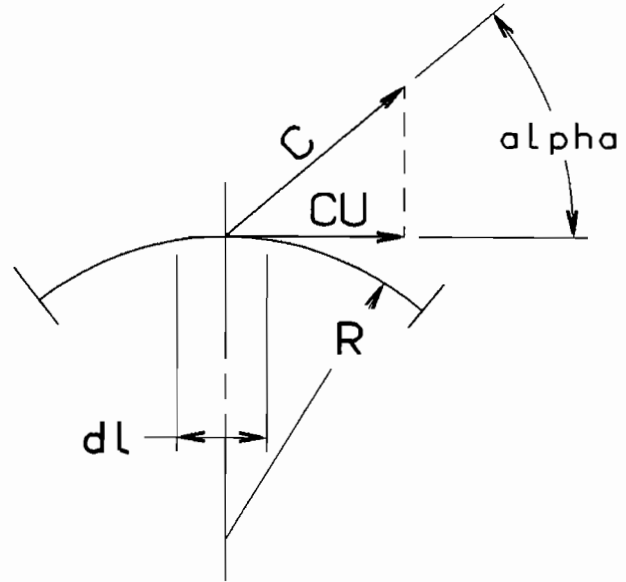$$\Gamma \text{ TOT} = [\Gamma (M) - \Gamma 1] = 2\pi [R(M) \cdot CU(M) - R1 \cdot CU1] \qquad (A\text{-}6)$$

Figure A-1. Definition of Circulation.

NOMENCLATURE

Symbols	Definition
BETA	Vane angles along meridional length
BETA 1	LE blade angle
BETA 2	TE blade angle
BF2	Flow angles along meridional length
CLINE	Center line
CM	Meridional velocity
CM (M)	Meridional velocity, at any point of meridional length
CU1	LE tangential velocity component
CU2	TE tangential velocity component, without slip
CU22	TE tangential velocity component, with slip
CU (M)	Tangential velocity component, at any point of meridional length
C (M)	Absolute velocity, at any point of meridional length
DH	Hub diameter
G	Gravity constant
H	Head
H THEO	Theoretical head
ILINE	Inside line, hub
LE	Leading edge
OLINE	Outside line, shroud
P	Pfleiderer slip factor
RS	Shroud radius
RW5	Blade diffusion rate
R1	LE radius
R2	TE radius
TE	Trailing edge
U1	LE peripheral velocity
U2	TE peripheral velocity
U (M)	Peripheral velocity at any point of meridional length
VL	Vane length
W	Relative velocity
WRAP	Length of vane in degrees

W9MIN   Minimum pressure slide blade velocity
W (M)   Relative velocity, at any point of meridional length
ZI   Number of vanes
Γ   Circulation, See Equation (5)
ω   Angular velocity Omega

REFERENCES

1. Stepanoff, A. J., *Centrifugal and Axial Flow Pumps*, New York: John Wiley and Sons (1948).

2. Pfleiderer, C., "Die Kreisel Pumpen," Springer Verlag (1961).

3. Viteri, F., "Computer Aided Design of Impellers," Pump Short Course, Turbomachinery Laboratory, Department of Mechanical Engineering, Texas A&M University, College Station, Texas (1983).

4. Borges, J. E., "A Three-Dimensional Inverse Method in Turbomachinery," ASME Papers 89-GT-136 & 137, Part I and II (1989).

5. Ghaly, W. S. and Tan, C. S., "A Parametric Study of Radial Turbomachinery Blade Design in Three-Dimensional Subsonic Flow," ASME paper 89-GT-84 (1989).

6. Katsanis, T., "Quasi Three-Dimensional Flow Analysis in Turbomachinery: A Tool for Blade Design," ASME. FED 120, ASME/JSME Fluids Engineering Conference, Portland, Oregon (1991).

7. Stanitz, J. D., "Design of Two-Dimensional Channels with Prescribed Velocity Distribution Along the Channel Walls," NACA Report-1115, (1953).

8. Bonataki, E., Chaviaropoulus, P., and Papailiou, K. D., "An Inverse Method for the Design of Quasi-Three Dimensional Turbomachinery Cascades," FED 120, ASME/JSME Fluids Engineering Conference, Portland, Oregon (1991).

9. Al-Zubaidy, S. N. J., "A Refined Analytical Method for Designing High Pressure Ratio Centrifugal Impellers," FED 120, ASME/JSME Fluids Engineering Conference, Portland, Oregon (1991).

10. Spring, H., "The Impeller Inlet, Methods to Justify Proper Selection for Pumps," ASME Paper No. 84WA/FM-1 (1984).

11. Spring, H., "A Comprehensive Streamline Theory Based Euler, with Pfleiderer's Modification for Slip and Hydraulic Efficiency, Suitable for Pumps with Prerotation," ASME FED, 6, Boston, Massachusetts (1983).

12. Morris, R. E. and Kenny, P. D., "High Pressure Ratio Centrifugal Compressors for Small Gas Turbine Engines," in Advanced Centrifugal Compressors, ASME (1971).

13. Spring, H., "Critique of Three Boiler Feed Pump Suction Impellers," Pumping Machinery, ASME FED, 81, (1989).

14. Schiavello, B. and Sen, M., "On the Prediction of Reverse Flow Onset at the Centrifugal Pump Inlet," ASME Symposium Performances Prediction of Centrifugal Pumps and Compressors, New Orleans, Louisiana (1980).

15. Kovats A. and Desmut G., *Pumps, Fans and Compressors*, London: Blackie and Son, Limited (1958).

16. Yedidiah, S., "About the Validity of a Slip-Factor for Predicting the Head of a Centrifugal Pump," FED 120, ASME/JSME Fluids Engineering Conference, Portland, Oregon (1991).

17. Stepanoff, A. J., *Pumps and Blowers*, New York: John Wiley and Sons, (1964).

ACKNOWLEDGEMENT